Molecular-dynamics study of solid γ-O_2

Michael L. Klein
Chemistry Division, National Research Council of Canada, Ottawa, Canada K1A OR6

D. Levesque and J.-J. Weis
Laboratoire de Physique Théorique et Hautes Energies, Université Paris-Sud, 91405 Orsay, France*

(Received 4 February 1980)

A molecular-dynamics study of the structure and dynamics of solid γ-O_2 has been carried out using a system of 512 molecules interacting via atom-atom potentials. As in the real solid, our simulated crystal is composed of two types of molecules whose dynamical behavior is quite distinct. The γ-phase dynamical structure factor $S(\vec{Q},\omega)$ has been examined at two densities. A simulation for the liquid, close to the triple point, has been carried out to compare and contrast with the solid.

I. INTRODUCTION

When oxygen solidifies from the liquid it forms a plastic crystal whose structure is depicted in Fig. 1. This so-called γ phase is a cubic structure with eight molecules in the unit cell.[1] The structure, which is analogous to the famous A-15 structure of high-temperature superconductors, is best visualized as being composed of linear chains of orientationally disordered "disk-like" molecules running along the ⟨001⟩ directions (molecules 2–6 of Fig. 1) with "spherically" disordered molecules (1 and 8) lying on an interpenetrating body-centered-cubic lattice. At zero pressure the γ phase exists between 43.8 and 54.4 K. In this interval the lattice parameter has been measured by x rays.[2,3] A more recent neutron-diffraction study[4] revealed that the "spherically" disordered molecules were actually preferentially oriented along the ⟨111⟩ directions. The equation of state,[5] the heat capacity,[6] and the polycrystalline sound velocities[7] have been reported. The Raman spectrum[8] of the γ-phase solid and the liquid[9] consists of a broad wing on the side of the Rayleigh line that extends to around 100 cm^{-1} with a bump around 40 cm^{-1}. There thus appears to be great similarity between the molecular reorientational dynamics in these two phases. Brillouin spectroscopy has been used to determine the elastic constants of single crystals.[10] Since both the longitudinal and transverse Brillouin shifts depended little on the crystal orientation, it was concluded that γ-O_2 is elastically isotropic. At the triple point (54.4 K) the longitudinal sound speed is about 15% greater in the solid than in the liquid.[11] Apart from the elastic isotropy, the other unusual feature of the γ phase is the ratio of the longitudinal sound speed v_l to the transverse speed v_t which is more than a factor of 3 (Refs. 7 and 10). This is to be contrasted with hexagonal-close-packed solid β-N_2 where this ratio is about 2 (Ref. 7), and a typical rare-gas crystal[12] where the ratio is about 1.5. The reason is that the shear constant of this plastic crystal is anomalously low. The translational lattice frequencies have been calculated[13] using an empirical force-constant model. This model which completely neglects the effect of molecular rotation was able to account for the low shear constant of γ-O_2 but not the elastic isotropy. This is the only theoretical work reported to date.

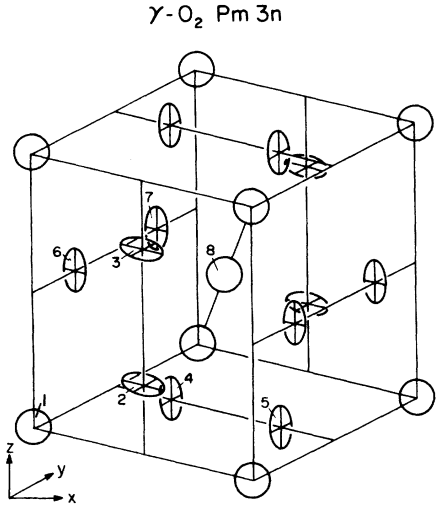

FIG. 1. The crystal structure of γ-O_2. The "disk-like" molecules (2–6) have site symmetry D_{2d}, while the "spherical" molecules (1, 8) have site symmetry T_h and are preferentially oriented in ⟨111⟩ directions.

In the present paper we present a classical computer-simulation molecular-dynamics (MD) experiment for the γ and liquid phases. We hope by this means to examine in more detail the role played by the molecular reorientational motions in the crystal dynamics and also to contrast the behavior of molecules in the plastic phase with

those in the liquid. The organization of the paper is as follows. The interatomic force model is discussed in Sec. II. Section III presents details of the calculations. Section IV gives the power spectra associated with the self-correlation functions describing the molecular motions. Finally, in Sec. V we present results for the dynamical structure factor $S(\vec{Q},\omega)$ of γ-O_2.

II. INTERMOLECULAR POTENTIAL

Following previous work on the lattice dynamics of the low-temperature-ordered α and β crystal phases,[13,14] we employ an atom-atom potential

$$V(R) = 4\epsilon\left[(\sigma/R)^{12} - (\sigma/R)^{6}\right], \tag{1}$$

with fixed half-bond length $d = 0.2021\sigma$. The previous studies used $\epsilon/k_B = 58$ K, $\sigma = 2.988$ Å, and $d = 1.2076$ Å (Ref. 14). We will refer to these parameters as "solid-state" parameters. We will not introduce the quadrupole moment of O_2 since it is known to be small.[15] Moreover, the increased bond length of the O_2 molecule with respect to N_2 suggests that the atom-atom approach should be more reasonable here. Figure 2 shows potential energy curves for the energetically more favorable dimer configurations. The figure

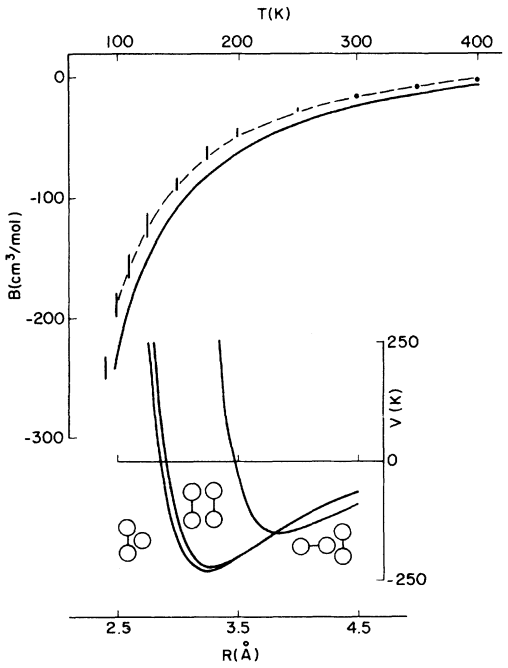

FIG. 2. The lower portion of the figure shows selected dimer potential energy curves calculated using Eq. (1) of the text and "solid-state" parameters. The upper portion shows the second virial coefficient of the gas. The full line is calculated for the solid-state potential, the dashed line for the "gas-phase" parameters. The data are taken from Ref. 17.

demonstrates that this potential function is not entirely adequate since the global minimum arises for the crossed rather than the parallel dimer configuration known to arise experimentally.[16] However, the difference in energy between these two structures is only about 6 K at their respective minima. Since we will be interested in the solid γ phase and liquid phase at much higher temperatures, the energy difference between these two configurations will become unimportant.

The second virial coefficient $B(T)$ of gaseous O_2 based upon the "solid-state" potential given above is shown in Fig. 2 (solid line) along with selected experimental data.[17] The agreement with experiment is not particularly good. We note in passing that an essentially perfect fit to $B(T)$ can be achieved with $\epsilon/k_B = 52$ K (dashed line Fig. 2). An almost equivalent fit would be obtained using $\epsilon/k_B \sim 51$ K and $\sigma \sim 3.02$ Å. We will refer to this latter set of parameters as "gas-phase" parameters.

III. DETAILS OF THE CALCULATIONS

For our MD calculations on solid γ-O_2 we employed a system of 512 molecules whose centers of mass were arranged in the A-15-type structure (Fig. 1). This system consisted of 64 unit cells ($4\times4\times4$) of 8 molecules each. "Disk-like" molecules (2–6 in Fig. 1) were given initial random $\langle 110\rangle$ orientations and "spherical" molecules (1 and 8 in Fig. 1) were given random $\langle 111\rangle$ orientations. Periodic boundary conditions were used to simulate an infinite system. The basic MD program was the same as used previously in our study of solid and liquid N_2.[18,19] The molecules interacted with the atom-atom potential quoted above but truncated for $R > 2.63\sigma$. The motion of the 512 molecules was simulated for 3 state conditions; the basic data are given in Table I. The MD calculations are classical and it is natural to use the reduced quantities given in Table I. In order to convert to absolute quantities we have used the "solid-state"-potential parameters,[13,14] and also those obtained from fitting to the second virial coefficient of the gas (Sec. II). We see from Table I that for both the liquid and the low-density plastic γ phase, the pressure was computed to be negative. The most recent x ray work[3] shows that the molar volume of γ-O_2, under its own vapor pressure, ranges from 22.9 cm^3/mol at 44 K to about 23.5 cm^3/mol at 54 K. Thus the gas-phase parameters would seem to be the better set of parameters. Nevertheless, for consistency with previous work on the solid[13,14] we will use "solid-state" parameters throughout the

TABLE I. Summary of MD data for solid γ and liquid phases. To convert reduced quantities to absolute values we have used $\epsilon/k_B = 58$ K and $\sigma = 2.988$ Å (Refs. 13 and 14). Values for $\epsilon/k_B = 51$ K $\sigma = 3.02$ Å are given in parentheses.

Phase	System size N	Density $\rho^* = N\sigma^3/V$	Temperature $T^* = k_BT/\epsilon$	$Z = pV/Nk_BT$	$\rho_{\vec{\tau}}$ [b]
γ-O_2	512	0.70	1.02	−2.6	~250
γ-O_2	512	0.80	1.20	+15.7	~300
l-O_2	512	0.64	1.30	−2.5	~0

Phase	V (cm^3/mol)	T (K)	$\langle(R-R^0)^2\rangle$ Å^2	p (kbar)	⟨PE⟩ (kcal/mol)	D (10^{-5} cm^2/s)
γ-O_2	22.95(23.65)	59.2(52.0)	0.28	−0.56	−2.18	
γ-O_2	20.08(20.69)	69.6(61.2)	0.20 [a]	+4.52	−2.20	
l-O_2	25.10(25.86)	75.4(66.3)		−0.63	−1.98	1.3

[a] The component contributions are $\langle(R_\alpha - R_\alpha^0)^2\rangle_s = 0.073$ Å^2, $\langle(R_\alpha - R_\alpha^0)^2\rangle_\perp = 0.072$ Å^2, and $\langle(R_\alpha - R_\alpha^0)^2\rangle_\parallel = 0.046$ Å^2 for the spherically disordered and chain-like molecules, respectively ($\alpha = x$, y, or z).

[b] We have used $\vec{\tau} = 2\pi(1, 0, 0)/a$.

remainder of this paper.

We see from Table I that in the low-density solid, the mean-square amplitude of vibration of the molecular centers of mass is about 0.28 Å^2, which corresponds to about 16% of the closest intermolecular distances. This value was found to be quite stable throughout the MD calculations for the γ phase, indicating that our simulated system was indeed a solid. Moreover, we also monitored

$$\rho_{\vec{\tau}} = \sum_{j=1}^{N} \exp(i\vec{\tau}\cdot\vec{R}_j),$$

where $\vec{R}_j$ are the position vectors of the molecular centers of mass, and $\vec{\tau}$ is a vector of the reciprocal lattice of the crystal. The structure amplitude $\rho_{\vec{\tau}}$ was calculated to be about 250 and reasonably constant, again indicating that we had simulated a solid.

In addition to the thermodynamic properties, we have calculated certain self-time-correlation functions for both the liquid and plastic phase and these will be discussed in Sec. IV. Finally, we carried out two longer runs each of more than 20 000 steps (5×10^{-15} s) for the γ phase. These runs were used to calculate the dynamical structure factor $S(\vec{Q}, \omega)$, and this also will be discussed in detail in Sec. IV.

IV. RESULTS

A. Structure of the γ phase

The relevant information on the structure is contained in the angle-averaged *atomic* radial distribution function $g(r)$. This quantity is shown in Fig. 3 for both the solid γ and liquid phases. The similarity of the two $g(r)$'s is remarkable. In the solid phase the main peak around 1.1σ is clearly due to nearest-neighbor molecules along the chain directions (for example R_{23}, R_{45}, and R_{67} in Fig. 1). The shoulder on the side of the main peak at around 1.35σ, arises from interatomic distances occurring in R_{24} and R_{25}, etc. The second peak in $g(r)$, around 2.15σ, arises mainly from pairs of molecules R_{34}, R_{35}, etc.

The peaks in $g(r)$ are clearly insufficient to characterize the solid γ-phase structure since we have seen that the liquid has a virtually indistinguishable $g(r)$. Accordingly, we have also

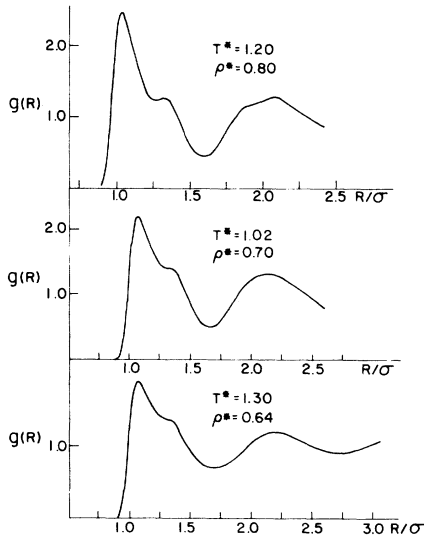

FIG. 3. Atomic radial distribution functions $g(R)$ for solid γ-O_2 and the liquid.

examined correlation functions of the type

$$C_{\alpha\beta}(t) = \langle u_\alpha(t) u_\beta(0) \rangle ,$$

where $\vec{u}$ is unit vector along the molecular symmetry axis and α and β refer to the crystal axes x, y, and z shown in Fig. 1. Table II gives the values of this function for $t = 0$. We have averaged over the appropriate pairs of molecules; thus molecules 1 and 8 are paired as are (2, 3), (4, 5), and (6, 7). The most striking feature of our results (see Table II) is that the bond vectors for molecules (1, 8) behave quite differently from the other pairs such as (2, 3). Indeed, the description of molecules (1, 8) as "spherical" and (2, 3) as "disk-like" is quite appropriate. Of course, strictly, for the (1, 8) pair we cannot use Table II to distinguish between spherical disorder or random ⟨111⟩ orientations. A detailed study of the motion of individual molecules selected at random from the system reveals that the "disk-like" molecules of type 2 or 3 in Fig. 1 rarely move out of the xy plane by more than 30° while the "spherical" molecules (type 1 and 8 in Fig. 1) show a slight preference for ⟨111⟩ orientations. We therefore seem to have simulated the γ phase in our MD calculations.

B. Self-correlation functions

We have examined the self-time-correlation functions that are readily evaluated from the phase-space trajectories of the MD calculations. In particular, for the liquid, we have studied the velocity autocorrelation function

$$Z(t) = \langle \vec{V}(t) \cdot \vec{V}(0) \rangle / \langle \vec{V}(0) \cdot \vec{V}(0) \rangle$$

TABLE II. Components of $\langle u_\alpha(0) u_\beta(0) \rangle$ for solid γ-O_2 where $\vec{u}$ is a unit vector along the molecular symmetry axis. The axes and molecules are labeled as in Fig. 1.

	$T^* = 1.02$		$\rho^* = 0.70$	
$\alpha\beta$	(1, 8)	(2, 3)	(4, 5)	(6, 7)
xx	0.341	0.442	0.106	0.443
yy	0.330	0.451	0.444	0.105
zz	0.329	0.107	0.450	0.452
xy	−0.002	−0.012	0.005	0.002
xz	0.003	0.001	−0.001	0.002
yz	0.004	−0.001	0.001	0.002
	$T^* = 1.20$		$\rho^* = 0.80$	
xx	0.327	0.464	0.074	0.465
yy	0.336	0.459	0.464	0.074
zz	0.337	0.076	0.461	0.462
xy	0.010	−0.002	0.004	0.003
xz	0.010	0.002	0.003	−0.013
yz	−0.007	−0.006	0.014	0.001

and its associated power spectrum

$$Z(\omega) = \int_0^\infty Z(t) \cos\omega t \, dt .$$

The latter is shown in Fig. 4. The self-diffusion coefficient for molecules in the fluid can be estimated from Fig. 4 to be 1.3×10^{-5} cm²/s. In the case of the γ phase, we have evaluated separately the velocity autocorrelation function for spherical (T_h) and disk-like (D_{2d}) molecules. The latter has also been separated into components parallel and perpendicular to the chain directions. These we label $Z_\parallel(t)$ and $Z_\perp(t)$ while this function for spherical (T_h) molecules is labeled $Z_s(t)$. The time correlations are not shown explicitly here but Fig. 4a gives the power spectra $Z_\parallel(\omega)$, $Z_\perp(\omega)$, and $Z_s(\omega)$ for the low-density γ phase. We see that these spectra are all quite different in character and only $Z_\perp(\omega)$ resembles at all the $Z(\omega)_{I_1}(t)$

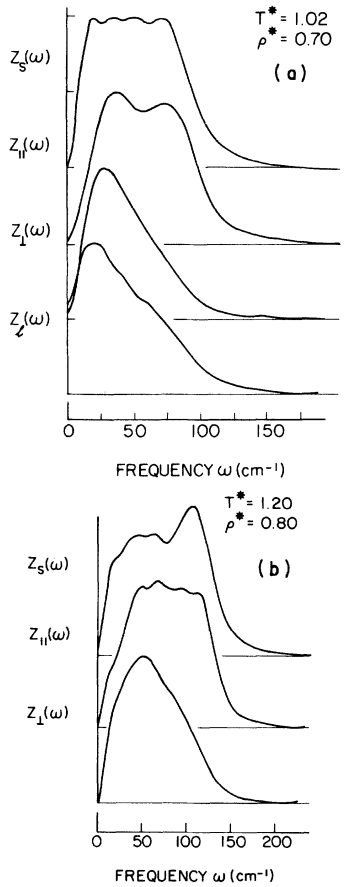

FIG. 4. The power spectra of the velocity autocorrelation functions $Z(\omega)$ for (a) $T^* = 1.02$, $\rho^* = 0.70$ and (b) $T^* = 1.20$, $\rho^* = 0.80$. The subscripts have the following meaning: s-"spherical" (T_h molecules), l-liquid, $\perp$ and $\parallel$-"disk-like" (D_{2d}) molecules perpendicular and parallel to the chain directions (see Fig. 1).

for the liquid. We recall that for a harmonic crystal, $Z(\omega)$ is nothing more than the density of vibrational (phonon) states involving motions of the centers of mass. Here we see that translational motions have spectra that span the range up to around 120 cm^{-1}, with the main peaks occurring between 20 and 75 cm^{-1}.

The liquid $Z(\omega)$ has a peak around 20 cm^{-1} and a broad shoulder at 70 cm^{-1}. The peaks in $Z_{\parallel}(\omega)$ occur at 35 and 75 cm^{-1}, while for $Z_{\perp}(\omega)$ they are around 30 and 70 cm^{-1}, similar to the liquid. Finally, peaks in $Z_s(\omega)$ arise at 20, 35, 50, and 70 cm^{-1}. The latter values appear to correlate reasonably well with previous lattice dynamical calculations[13] of the translational lattice modes which suggest peaks in this range. At higher pressure the power spectra behave in essentially the same fashion except that peak positions shift to higher frequencies. For example, the high frequency in $Z_s(\omega)$ is now around 115 cm^{-1} rather than 70 cm^{-1} [see Fig. 4(b)].

We have also calculated the analogous autocorrelation functions associated with motion of the bond vectors (reorientational motion). Thus we have evaluated quantities such as $C(t) = \langle \vec{u}(0) \cdot \vec{u}(t) \rangle$ for the liquid, along with $C_{\parallel}(t)$, $C_{\perp}(t)$, and $C_s(t)$ for the γ phase. The associated power spectra $C_l(\omega)$, $C_{\parallel}(\omega)$, $C_{\perp}(\omega)$, and $C_s(\omega)$ are shown in Fig. 5. Except for $C_{\parallel}(\omega)$, which reflects the rocking motions of "disk-like" (D_{2d}) molecules along the chain direction, the power spectra decay rapidly. The spectra $C_s(\omega)$ and $C_l(\omega)$ are nearly indistinguishable indicating that for these molecules the reorientational motions are similar, while the decay of $C_{\perp}(\omega)$ is even more rapid than either of these. Thus the easiest reorientational motion is for the "disk-like" (D_{2d}) molecules perpendicular to the chain directions. The high-density γ-phase results are shown by the dashed lines in Fig. 5. The initial decay of these functions is always more rapid; however, $C_{\parallel}(\omega)$ now extend to higher frequencies.

Finally, we have calculated the correlation function appropriate to Raman scattering, namely, $I_l(t) = \langle P_2[\vec{u}(0) \cdot \vec{u}(t)] \rangle$. For the liquid, the power spectra $I_l(\omega)$ is given in Fig. 6 along with the analogous functions for the solid phase. Here we have separated the contributions of the "spherical" molecules (1, 8) [shown as $I_s(\omega)$] from that of the other molecules $I_d(\omega)$. The spectra are all very similar. As before, we show the high-density-solid results as dashed lines. The most striking feature of the $I(\omega)$ is that they all show a definite change of slope in the middle of spectral range (around 20 to 40 cm^{-1}). These spectra look somewhat similar to the data reported for the Raman spectra[8] of γ-O_2, but do not extend over a wide enough range of frequency. This would seem to imply that the mean-square torques are too small in our model. It also raises the question of the possible contribution of non-self-terms[19] being responsible for the observed bump in the experimental Raman spectrum.

C. Dynamical structure factor

One of the main objectives of our MD study was to examine the nature of the collective modes in the plastic crystal phase. The appropriate quantity to examine is $S(\vec{Q}, \omega)$, the van Hove function, where $\vec{Q}$ is the momentum transfer and ω the

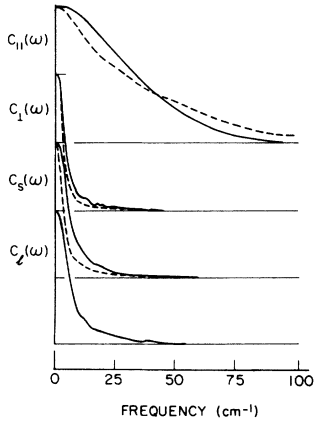

FIG. 5. The power spectra associated with reorientational motion $C(\omega)$. The subscripts have the same meaning as in Fig. 4. The solid lines are for the liquid and the low-density γ phase. The dashed lines are for the high-density γ phase.

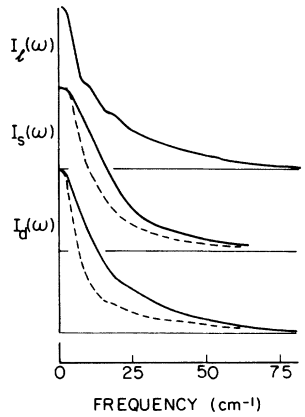

FIG. 6. The power spectra associated with Raman scattering $I(\omega)$. The contribution from D_{2d} molecules is indicated by the subscript d, that from the liquid by l, and that from the T_h molecules by s. The high-density γ-phase spectra are shown as dashed lines.

energy transfer to the solid. In detail we obtain the dynamical structure factor from

$$S(\vec{Q},\omega)=\int_0^\infty F(\vec{Q},t)\cos\omega t\,dt\,,$$

where the intermediate scattering function is

$$F(\vec{Q},t)=\frac{1}{4N}\sum_{i,j}^{N}\langle\rho_i(\vec{Q},t)\rho_j^*(\vec{Q},0)\rangle\,.$$

The density operators are written

$$\rho_i(\vec{Q},t)=2\exp[i\vec{Q}\cdot\vec{R}_i(t)]\cos[d\vec{Q}\cdot\vec{u}_i(t)]\,,$$

where, as before, $\vec{R}_i$ is the position vector of the molecule center of mass, and $\vec{u}$ is a unit vector along the molecule symmetry axis. N is the number of molecules in the system and d is the half-bond length.

We have evaluated $F(\vec{Q},t)$ along with the similar quantity for the centers of mass. The latter is obtained by setting the cosine term in the equation for ρ to unity.

Our system size, $4\times4\times4$ unit cells, and the periodic boundary condition, restricts the allowed values of $\vec{Q}$ to be of the form

$$\vec{Q}=(2\pi/4a)(l,m,n)\,,$$

where l, m, and n are integers and a is the cubic lattice constant of the γ phase. Figure 7 shows some representative $S(\vec{Q},\omega)$ spectra for the $\langle110\rangle$ and $\langle111\rangle$ directions of the low-density solid. The spectra are indexed by the integers (lmn). Spectra for the $\langle100\rangle$ behave similarly. The first point to note is that the spectra for longitudinal modes propagating in the $\langle100\rangle$, $\langle110\rangle$, and $\langle111\rangle$ directions have peak positions in the ratio 1:1.37:1.65. For an elastically isotropic solid we would expect the ratios to be $1:2^{1/2}:3^{1/2}$. With due allowance

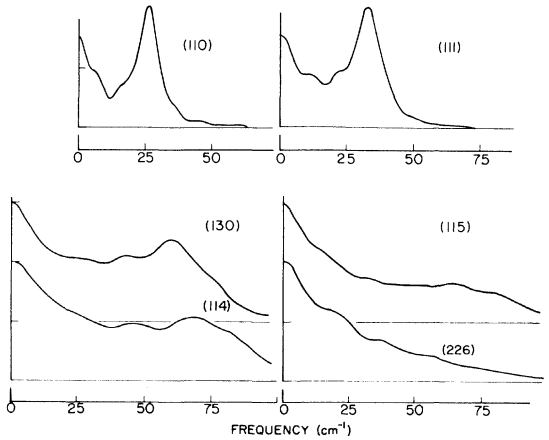

FIG. 7. Dynamical structure factor $S(\vec{Q},\omega)$ for the low-density γ phase. The curves are labeled by the integers (lmn) where $\vec{Q}=2\pi(l,m,n)/4a$.

for the possible effect of dispersion and the uncertainty in the calculated peak positions, we conclude that the low-density solid is indeed elastically isotropic. The mean velocity of longitudinal sound v_l, is 1.6×10^5 cm/s, which is about 10% higher than the corresponding experimental value.[7,10] In this regard we note that use of the "gas-phase potential" of Sec. II would result in the frequency scales of Figs. 4–7 being reduced by a factor of 0.928. The sound speed would then agree rather well with the experimental value of v_l. Based upon the experimental ratio $v_l/v_t\sim3$ (Refs. 7 and 10), we estimate that the transverse acoustic phonon peaks should occur at 9 and 11 cm^{-1} for the (114) and (115) spectra shown in Fig. 7. No such peaks are observed. Instead, in this region these spectra are dominated by broad quasielastic "central peaks" due to the rotational diffusion of the O_2 molecules. The situation here is quite similar to the case of β-N_2 (Ref. 18). In the $\langle110\rangle$ direction the broad features present in the (130) and (114) spectra between 25 and 30 cm^{-1} and between 40 and 50 cm^{-1}, as well as the high-frequency peaks at 60 and 70 cm^{-1}, all correlate well with the translational lattice modes predicted on the basis of lattice dynamical calculations.[13] The same conclusion applies to the (115) and (226) spectra and those for the $\langle100\rangle$ direction which are not shown in Fig. 7. In summary, it seems that the translational lattice modes give rise to those features that are seen in the $S(\vec{Q},\omega)$ spectra. However, the rotational diffusion of the molecules which dominates the low-frequency response prohibits the resolution of the transverse acoustic phonons. It is difficult for us to know whether this is an artifact of our MD simulation or a feature intrinsic to γ-O_2. In order to help clarify this situation, we carried a calculation of $S(\vec{Q},\omega)$ for a higher-density solid (see Table I) also. Our hope was that the increased density would shift the transverse acoustic phonons to sufficiently high frequency for a given $\vec{Q}$ vector that they would be separated from the "central peak" due to rotational diffusion. The latter should also narrow and hence enhance the possibility of observing the transverse acoustic modes.

Figure 8 shows some $S(\vec{Q},\omega)$ spectra for the high-density γ-O_2. The longitudinal acoustic modes in the $\langle100\rangle$, $\langle110\rangle$, and $\langle111\rangle$ directions are in the ratios 1 :1.36 :1.67, much the same as found in the low-density solid. However, the peak positions have shifted by approximately 60%. Inspection of Fig. 8 reveals the presence of additional low-frequency peaks that cannot be indexed on the basis of uniformly scaling by 60%, features present in the corresponding low-density

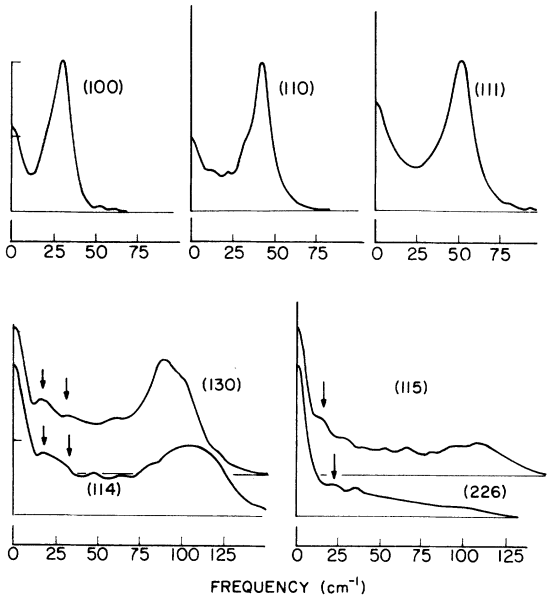

FIG. 8. Dynamical structure factor $S(\vec{Q}, \omega)$ for the high-density γ phase. The curves are labeled by integers (lmn) where $\vec{Q} = 2\pi(l, m, n)/4a$. The arrows indicate peaks due to transverse acoustic phonons.

data of Fig. 7. These additional peaks are indicated by arrows. The spectra (115) and (226) for modes propagating along the ⟨111⟩ direction each reveal an additional peak which clearly shows dispersion. These peaks at 15 and 23 cm^{-1} we identify as the transverse acoustic phonon. Based upon the peak position for the longitudinal mode propagating (see Fig. 8) in this direction, we estimate $v_l/v_t \sim 3.5$ in fair agreement with experiment.[7,10] The $S(\vec{Q}, \omega)$ spectra for transverse modes propagating along the ⟨100⟩ direction are not shown in Fig. 8 explicitly but, for example, the lowest frequency peak resolved for the point (240) is at about 19 cm^{-1}, which is consistent with our interpretation of the spectra for the ⟨111⟩ direction. With this identification plus the assumption of elastic isotropy, we would expect a peak around 12 cm^{-1} for the phonons (130) and (114). Unfortunately, this peak does not appear to be present. Instead, there are now two additional peaks in the spectra (130) and (114), the best resolved of which is around 18 cm^{-1}, somewhat higher than expected. The overall similarity of these two spectra seems to confirm the notion of elastic isotropy but a complete assignment of these peaks is not possible.

The simulated $S(\vec{Q}, \omega)$ spectra for the transverse modes are always dominated by the highest-frequency translational mode at high energy and a central peak due to rotational diffusion at low energy. In the intermediate energy range there are additional bumps (peaks) due to acoustic phonons and other translational modes. It is clear that in the simulation there are low-frequency transverse acoustic phonons, but they are not well resolved and hence a detailed analysis in terms of elastic constants is not worthwhile. There seem to be no peaks due to collective reorientational motions.

V. SUMMARY

We have carried out a computer simulation of both the plastic γ phase and the liquid oxygen using a simple atom-atom potential model. The γ phase has been found to be stable. Our study reveals the broad features of the dynamical behavior of the two distinct types of molecules in this structure. The liquid has been shown to be very similar in structure and dynamical behavior to the plastic phase. Finally, $S(\vec{Q}, \omega)$, the dynamical structure factor, has been examined and shown to consist of broad and often ill-defined spectra. The study of the high-density γ-O_2 helped identify very slow transverse acoustic phonons propagating in this solid. While there is fair agreement with experimental data on the sound speeds, certain features of the $S(\vec{Q}, \omega)$ data are not fully understood. It would be of considerable interest to have an experimental study of the inelastic neutron scattering from solid γ-O_2. Such data would not only test our predictions for $S(\vec{Q}, \omega)$, but would no doubt also help refine the intermolecular force model.

ACKNOWLEDGMENTS

This work was supported in part by the CNRS-NRCC exchange agreement. M. L. K. would like to thank Harry Kiefte and Maynard Clouter for enlightening conversations.

*Laboratoire associé au Centre National de la Recherche Scientifique.

[1]T. H. Jordan, W. E. Streib, H. W. Smith, and W. N. Lipscomb, Acta Crystallogr. 17, 777 (1964).
[2]C. S. Barrett, L. Meyer, and J. Wasserman, Phys. Rev. 163, 851 (1967).
[3]I. N. Krupskii, A. I. Prokhvatilov, Yu. A. Freiman, and A. I. Erenburg, Sov. J. Low Temp. Phys. 5, 130 (1979).
[4]D. E. Cox, E. J. Samuelsen, and K. H. Beckurts, Phys.

Rev. B 7, 3102 (1973).
[5]R. Stevenson, J. Chem. Phys. 27, 673 (1957); J. W. Stewart, J. Phys. Chem. Solids 12, 122 (1959).
[6]C. H. Fagerstrom and A. C. Hollis-Hallet, J. Low Temp. Phys. 1, 3 (1969).
[7]P. A. Bezuglyi, L. M. Tarasenko, and Yu. S. Ivanov, Sov. Phys.—Solid State 10, 1660 (1969).
[8]J. E. Cahill and G. E. Leroi, J. Chem. Phys. 51, 97 (1969).
[9]M. Blumenfeld, Nat. Bur. Stand. (U.S.) Spec. Publ. 301, 441 (1969).
[10]H. Kiefte and M. J. Clouter, J. Chem. Phys. 62, 4780 (1975).
[11]M. J. Clouter and H. Kiefte, J. Chem. Phys. 59, 2537 (1973).
[12]B. P. Stoicheff, in *Rare Gas Solids*, edited by M. L. Klein and J. A. Venables (Academic, New York, 1977), Vol. II, p. 979.
[13]K. Kobashi, M. L. Klein, and V. Chandrasekharan, J. Chem. Phys. 71, 843 (1979).
[14]J. C. Laufer and G. E. Leroi, J. Chem. Phys. 55, 993 (1971).
[15]A. Koide and T. Kihara, Chem. Phys. 5, 34 (1974).
[16]C. A. Long and G. R. Ewing, J. Chem. Phys. 58, 4824 (1973).
[17]J. H. Dymond and E. B. Smith, *The Virial Coefficient of Gases* (Clarendon, Oxford, 1969).
[18]M. L. Klein and J. -J. Weis, J. Chem. Phys. 67, 217 (1977); 63, 2869 (1975).
[19]J. -J. Weis and D. Levesque, Phys. Rev. A 13, 450 (1976).